

STAR TBI BRAIN SCAN:

In the diagnosis of Traumatic Brain Injury (TBI), advanced brain imaging techniques play a crucial role in providing detailed insights into the extent and nature of the injury. Among these techniques, Susceptibility-Weighted Imaging (SWI), Fluid-Attenuated Inversion Recovery (FLAIR), Diffusion Tensor Imaging (DTI), and Volumetric Imaging using NeuroQuant are particularly valuable. Each modality offers unique capabilities: SWI is sensitive to microhemorrhages and vascular damage, FLAIR highlights brain lesions of gliosis/scarring and edema, DTI maps white matter integrity and axonal injury, and NeuroQuant provides precise volumetric analysis of brain structures. Together, these imaging methods offer a comprehensive approach to diagnosing and understanding TBI, allowing for more accurate assessments and targeted treatment strategies.

Diffusion Tensor Imaging (DTI)

Diffusion Tensor Imaging (DTI) tractography is a specialized MRI technique that maps the diffusion of water molecules in the brain, providing detailed information about the brain's white matter tracts. It is particularly useful in demonstrating axonal shearing injury, which is a form of traumatic axonal injury (TAI) often resulting from traumatic brain injury (TBI).

Mechanism of Axonal Shearing Injury

Axonal shearing occurs when the brain is subjected to rapid acceleration or deceleration forces, as well as some component of rotational forces. These forces cause the axons (long nerve fibers that connect different parts of the brain) to stretch and tear. This injury disrupts the normal function of the axons and can lead to significant neurological impairment.

How DTI Tractography Demonstrates Axonal Shearing Injury

1. **Altered Diffusion Metrics**:

- **Fractional Anisotropy (FA)**: DTI measures the directionality of water diffusion within the brain's white matter. Healthy axons exhibit statistically normal FA values because water diffuses along the length of the axons. In axonal shearing, the disruption of axonal integrity can lead to a decrease or sometimes an abnormal increase in FA, indicating damage to the white matter

tracts.

- **Mean Diffusivity (MD)**:** This metric represents the overall diffusion of water in all directions. In areas of axonal injury, MD may be increased due to the loss of structural barriers that normally restrict water movement.

2. **Tractography Visualization**:**

- DTI tractography uses diffusion data to reconstruct the pathways of white matter tracts in the brain. In cases of axonal shearing, the affected tracts may appear fragmented, disrupted, or show an abnormal trajectory. The visualization might reveal areas where the tracts have been severed or where their continuity is compromised.

3. **Identification of Specific Injured Tracts**:**

- DTI tractography can help identify specific white matter tracts that have been affected by axonal shearing. This can correlate with clinical symptoms, such as motor deficits, cognitive impairment, or sensory disturbances, depending on the location of the injury.

4. **Quantitative Analysis**:**

- By comparing the diffusion metrics in injured regions to those in unaffected areas or to normative data, clinicians can quantitatively assess the extent of axonal damage. This analysis can be crucial for diagnosing the severity of the injury and for monitoring recovery or the effectiveness of therapeutic interventions.

Clinical Relevance

DTI tractography provides a non-invasive way to detect and characterize axonal shearing injuries that may not be visible on conventional MRI. This makes it an essential tool in the assessment of traumatic brain injury, helping guide treatment decisions and providing prognostic information.

FLAIR (Fluid Attenuated Inversion Recovery) IMAGING:

FLAIR (Fluid-Attenuated Inversion Recovery) imaging is a specialized MRI technique that is particularly useful in diagnosing Traumatic Brain Injury (TBI). It helps in the following ways:

1. **Detection of Small Lesions**: FLAIR imaging is sensitive to changes in the brain's white matter and can detect small lesions, such as microhemorrhages, gliosis, or areas of edema, which may not be visible on conventional MRI sequences. These lesions are often associated with TBI and can indicate the presence of diffuse axonal injury (DAI).
2. **Identification of Cortical Contusions**: FLAIR imaging excels at identifying cortical contusions—bruises on the brain's surface caused by the impact during TBI. These appear as hyperintense (bright) areas on FLAIR images, making them easier to distinguish from surrounding brain tissue.
3. **Evaluation of Brain Edema**: FLAIR imaging suppresses the signal from cerebrospinal fluid (CSF), allowing for a clearer view of the brain parenchyma. This makes it easier to identify areas of brain edema (swelling) that are common in TBI, particularly in the early stages.
4. **Chronic Injury Detection**: In the chronic phase of TBI, FLAIR imaging can help identify long-term changes, such as gliosis or encephalomalacia (softening of brain tissue), which may result from previous injuries. These appear as hyperintense regions and provide evidence of past trauma.

In summary, FLAIR imaging aids in diagnosing TBI by detecting small lesions, identifying cortical contusions, evaluating brain edema, and detecting chronic injury changes, making it a valuable tool in both acute and long-term assessment of TBI.



Susceptibility-Weighted Imaging (SWI)

Susceptibility-Weighted Imaging (SWI) is an advanced MRI technique that is particularly effective in diagnosing Traumatic Brain Injury (TBI). It aids in the following ways:

1. **Detection of Microhemorrhages**: SWI is highly sensitive to the presence of blood products, making it particularly effective at detecting microhemorrhages, which are small bleeds in the brain often caused by diffuse axonal injury (DAI) in TBI. These microhemorrhages may not be visible on conventional MRI sequences.
2. **Visualization of Hemorrhagic Lesions**: SWI can clearly visualize larger hemorrhagic lesions, such as contusions or hematomas, which occur as a result of TBI. These lesions appear as areas of low signal (dark areas) on SWI, making them easy to identify and assess.
3. **Assessment of Vein Integrity**: SWI can also assess the integrity of small veins in the brain. In cases of TBI, damaged veins may be visible as abnormally dark areas on SWI, indicating vascular injury or venous congestion associated with the trauma.
4. **Identification of Calcifications and Iron Deposits**: SWI can distinguish between different tissue types, allowing for the identification of calcifications and iron deposits, which can be sequelae of brain injury. This capability helps in understanding the extent and nature of the injury.

In summary, SWI aids in diagnosing TBI by detecting microhemorrhages, visualizing hemorrhagic lesions, assessing vein integrity, and identifying calcifications and iron deposits, making it a powerful tool for evaluating both acute and chronic effects of brain trauma.

VOLUMETRIC BRAIN IMAGING (NEUROQUANT)

Volumetric brain imaging is a technique used to measure the volume of different brain structures. In the context of diagnosing Traumatic Brain Injury (TBI), it helps in the following ways:

1. ****Detection of Brain Atrophy****: TBI can lead to the loss of brain tissue, resulting in atrophy. Volumetric imaging allows for precise measurement of brain volume, enabling the detection of even subtle atrophy in specific regions which may be affected by TBI.
2. ****Detection of Brain Enlargement**** Volumetric brain MRI can reveal enlargement of certain brain structures in cases of Traumatic Brain Injury (TBI) by precisely measuring and comparing brain volumes to a normative database. This volumetric analysis allows for the detection of abnormal increases in brain or ventricular volume, which can indicate the presence of underlying damage and contribute to the diagnosis and management of TBI.
3. ****Identification of Hemorrhages and Contusions****: Volumetric imaging can reveal areas of hemorrhage (bleeding) or contusions (bruises) within the brain, which are common in TBI. These areas often show up as changes in volume or density, providing critical information for diagnosis.
4. ****Assessment of Diffuse Axonal Injury (DAI)****: While not as detailed as DTI, volumetric imaging can show indirect signs of diffuse axonal injury, such as the enlargement of ventricles or atrophy in white matter regions, reflecting the loss of axonal integrity.
5. ****Monitoring Changes Over Time****: Volumetric imaging can be used to track changes in brain volume over time, which is useful for monitoring the progression of injury, recovery, or the effects of therapeutic interventions.

In summary, volumetric brain imaging aids in diagnosing TBI by detecting brain atrophy, identifying hemorrhages and contusions, assessing diffuse axonal injury, and monitoring changes over time.

Patient: XXXXXXXX DOB:
30-Mar-1992
MRN#: 209098EVI



Demographics

Patient Name: First: XXXXX Middle: Last: XXXXX XXXXX
Date of Birth: [REDACTED] Gender: M MRN#:209098EVI
Date of Injury: Date of Service: 22-Nov-2024 12:40 PM
Referring Provider / Source: XXXXX, XXXXX

EXAM: Brain MRI with advanced neuro diagnostic imaging including diffusion tensor imaging (3D), VOLUMETRIC ANALYSIS OF THE BRAIN UTILIZING THE NEUROQUANT TRIAGE BRAIN ATROPHY PROTOCOL, and susceptibility-weighted imaging (SWI).

IMPRESSION:

In conclusion, the findings are abnormal and are consistent with those seen in patients who have experienced a traumatic brain injury, providing objective evidence of permanent brain injury as observed through advanced brain imaging techniques. The likelihood that these imaging results accurately reflect a brain injury is 100%. Overall, the findings are compatible with a severe brain injury more so on the right brain than the left.

Overall, the diffusion tensor imaging shows abnormalities consistent with microstructural changes in various parts of the brain, which are often associated with traumatic axonal injury. I do not observe any other specific findings that would indicate an alternative diagnosis. There are no signs of strokes, brain tumors, masses, inflammation, demyelination, infection, or congenital brain or structural anomalies.

33.3% :11 Out of 33 white matter tracts are statistically significant out of the normal range in terms of microstructural measurements. The majority of the abnormal white matter tracts are statistically abnormal are within the right hemisphere..

9 out of 13 the paired white matter tracts demonstrates statistically significant abnormal asymmetry. These suggest abnormal white matter tracts with asymmetry beyond the 95th percentile in the normal population, indicating statistically significant abnormalities that suggests asymmetric axonal dysfunction, commonly seen in cases of traumatic brain injury.

The tractography reveals irregularities, including reduced fiber density and disrupted fiber tracts, corresponding to areas with abnormal axonal microstructural properties of the brain. These findings contribute to the 2-D and 3-D imaging and modeling of axonal dysfunction commonly seen in traumatic axonal injury.

The patient has undergone a prior right sided craniotomy and cranioplasty. There is a chronic right-sided subdural hematoma measuring up to 13.71 mm, series 100 image 232, series 18 image 42, series 19 image 20. This results in subjacent mass effect on the right cerebral hemisphere but no midline shift. There is an adjacent subcutaneous fluid collection overlying the calvarium within the scalp which measures 11.8 cm in anterior posterior dimensions and nearly 7.8 cm in craniocaudal dimensions and up to 2 cm in mediolateral dimensions, series 18 image 31-54, series 19 image 13-43. This is concerning for an adjacent CSF leak with fluid collecting beneath the scalp.

There is significant abnormality on susceptibility weighted imaging with old blood products along the surface of the right cerebral hemisphere lining the sulci of the right temporal frontal and parietal lobes and to lesser extent the right occipital lobe, series 16 image 30-70. Consistent with hemosiderin staining from old subdural blood and subarachnoid hemorrhage. However, there are also several scattered foci of hemosiderin throughout the brain parenchyma much more present on the right side of the brain in the left and centered at the gray-white matter junction, series 15 image 29-63 compatible with diffuse post traumatic microhemorrhages and diffuse axonal shearing injury. There is extensive hemosiderin and old blood products in the right temporal pole and the right frontal lobe in the areas of posttraumatic encephalomalacia compatible with sequelae of hemorrhagic contusions and direct impaction injury with permanent liquefied brain tissue and scarring now present, series 15 image 38-60,

Patient: XXXXXXXX DOB:
30-Mar-1992
MRN#: 209098EVI



Demographics

Patient Name: First: XXXXX Middle: Last: XXXXX XXXXX
Date of Birth: [REDACTED] Gender: M MRN#:209098EVI
Date of Injury: Date of Service: 22-Nov-2024 12:40 PM
Referring Provider / Source: XXXXX, XXXXX

series 17 image 27-50. Is also focal encephalomalacia in the left gyrus rectus and supraorbital gyrus consistent with posttraumatic encephalomalacia and permanent liquefied brain tissue with scarring secondary to direct impaction injury, series 17 image 31-36. These findings are also seen on series 18 image 23-50 and series 19 image 7-23. There are multiple scattered white matter signal foci throughout the brain centered at the gray-white matter junction in a pattern and distribution most typical of posttraumatic gliosis and scarring related to axonal shearing injury. This is more so on the left than the right, series 17 image 34-35, 38, 39, 40-40 1-40 2-43, 47, 50-52. There is associated ex vacuo dilatation of the frontal horn of the right lateral ventricle.

NeuroQuant triage brain atrophy report results: These findings are abnormal and can be seen in the setting of posttraumatic brain loss as well as evidence of posttraumatic gliosis and scarring. The pattern and distribution can be seen in the setting of axonal shearing injury as well as direct impaction injury of the brain such as a coup/contrecoup injury (direct brain impact injury). The specific brain loss in the right frontal lobe corresponds to the areas of extensive encephalomalacia and posttraumatic liquefied brain tissue and scarring. There is also a statistically significant decreased brain volume in the right anterior cingulate gyrus which is posttraumatic. Other areas demonstrate increased brain volume suggesting underlying brain scarring related to trauma.

Clinical correlation with the patient's history, physical, and symptoms is recommended. Comparison to any prior brain imaging is recommended. If any prior brain imaging becomes available, a direct comparison to the study could be performed, and an addendum can be provided at that time.

HISTORY: Patient was struck in the right side of the head 05/22/24. Pain with headaches and difficulty with memory and speech abnormality. Difficulty with balance. Difficulty processing. Changes in the patient's personality and emotions. Posttraumatic headache.

TECHNIQUE: Multiplanar and multiweighted MR sequences of the brain were obtained including T1, T2, FLAIR, diffusion-weighted imaging, SWI [susceptibility weighted imaging] Sagittal 3-D-SPGR thin section double inversion recovery images of the brain were obtained per Cortech Laboratories recommended scanner settings. All DICOM images were processed via the Cortech Laboratories NEUROQUANT imaging protocol and algorithm system. NEUROQUANT general morphology report as well as NeuroQuant triage brain atrophy study reports were obtained and analyzed. The neural quadrant normative database encompasses patients from 3-100 years of age. There are a total of 4000 neurotypical control group subjects. All data is matched for age and gender. All segmentation and data were produced in a DICOM and graphical interface reviewed and interpreted for quality control.

All diffusion tensor imaging was evaluated using tract-based statistical analysis and analyzed utilizing FDA cleared Advantis Brainance DTI Software for clinical use. White matter tracts were analyzed for apparent diffusion coefficient, fractional anisotropy and asymmetry. This patient's DTI Data was compared to a normal database of 1355 neurotypical healthy control subjects between 19-83 years old. 51.3% female and 48.7% male. All measurements and data were produced in a graphical interface reviewed and interpreted for quality control.

COMPARISON: None.

Patient: XXXXXXXX DOB:

MRN#: 209098EVI



Demographics

Patient Name: First: XXXXX

Middle:

Last: XXXXX XXXXX

Date of Birth: [REDACTED]

Gender: M

MRN#:209098EVI

Date of Injury:

Date of Service: 22-Nov-2024 12:40 PM

Referring Provider / Source: XXXXX, XXXXX

FINDINGS:

The patient has undergone a prior right sided craniotomy and cranioplasty. There is a chronic right-sided subdural hematoma measuring up to 13.71 mm, series 100 image 232, series 18 image 42, series 19 image 20. This results in subjacent mass effect on the right cerebral hemisphere but no midline shift. There is an adjacent subcutaneous fluid collection overlying the calvarium within the scalp which measures 11.8 cm in anterior posterior dimensions and nearly 7.8 cm in craniocaudal dimensions and up to 2 cm in mediolateral dimensions, series 18 image 31-54, series 19 image 13-43. This is concerning for an adjacent CSF leak with fluid collecting beneath the scalp.

There is significant abnormality on susceptibility weighted imaging with old blood products along the surface of the right cerebral hemisphere lining the sulci of the right temporal frontal and parietal lobes and to lesser extent the right occipital lobe, series 16 image 30-70. Consistent with hemosiderin staining from old subdural blood and subarachnoid hemorrhage. However, there are also several scattered foci of hemosiderin throughout the brain parenchyma much more present on the right side of the brain in the left and centered at the gray-white matter junction, series 15 image 29-63 compatible with diffuse post traumatic microhemorrhages and diffuse axonal shearing injury. There is extensive hemosiderin and old blood products in the right temporal pole and the right frontal lobe in the areas of posttraumatic encephalomalacia compatible with sequelae of hemorrhagic contusions and direct impaction injury with permanent liquefied brain tissue and scarring now present, series 15 image 38-60, series 17 image 27-50. Is also focal encephalomalacia in the left gyrus rectus and supraorbital gyrus consistent with posttraumatic encephalomalacia and permanent liquefied brain tissue with scarring secondary to direct impaction injury, series 17 image 31-36. These findings are also seen on series 18 image 23-50 and series 19 image 7-23. There are multiple scattered white matter signal foci throughout the brain centered at the gray-white matter junction in a pattern and distribution most typical of posttraumatic gliosis and scarring related to axonal shearing injury. This is more so on the left than the right, series 17 image 34-35, 38, 39, 40-40 1-40 2-43, 47, 50-52. There is associated ex vacuo dilatation of the frontal horn of the right lateral ventricle.

Sinuses, middle ears and mastoid air versus are clear. Orbits are unremarkable.

Incidental note of a lipoma at the left skull base measuring 3.3 x 1.6 x 3.6 cm, series 18 image 8, series 54 image 108.

DIFFUSION TENSOR IMAGING ANALYSIS:

Please refer to the advanced diagnostic neuro imaging (ANDI REPORT) for full evaluation. The diffusion tensor imaging of this patient's brain was compared to a normative database of 1355 healthy subjects an age and gender matched control group. Below is a summary of the findings:

33.3% :11 Out of 33 white matter tracts are statistically significant out of the normal range in terms of microstructural measurements. The majority of the abnormal white matter tracts are statistically abnormal are within the right hemisphere..

These indicate abnormal white matter tracts that fall beyond the 95th percentile of the normal population, pointing to statistically significant abnormalities that suggest axonal dysfunction, which can occur in cases of traumatic brain injury.

Patient: XXXXXXXX DOB:

MRN#: 209098EVI



Demographics

Patient Name: First: XXXXX

Middle:

Last: XXXXX XXXXX

Date of Birth: [REDACTED]

Gender: M

MRN#:209098EVI

Date of Injury:

Date of Service: 22-Nov-2024 12:40 PM

Referring Provider / Source: XXXXX, XXXXX

9 out of 13 the paired white matter tracts demonstrates statistically significant abnormal asymmetry. These suggest abnormal white matter tracts with asymmetry beyond the 95th percentile in the normal population, indicating statistically significant abnormalities that suggests asymmetric axonal dysfunction, commonly seen in cases of traumatic brain injury.

The tractography reveals irregularities, including reduced fiber density and disrupted fiber tracts, corresponding to areas with abnormal axonal microstructural properties of the brain. These findings contribute to the 2-D and 3-D imaging and modeling of axonal dysfunction commonly seen in traumatic axonal injury.

VOLUMETRIC IMAGING: NEUROQUANT

General morphometry:

Asymmetry inferolateral ventricles with the right much larger than the left. This is pathologic from next vacuo dilatation. There is asymmetry in the pallidum which is likely pathologic.

A NeuroQuant triage brain atrophy study was conducted, revealing statistically significant decrease in brain volume in the following segments, which fall below the 5th percentile compared to a database of normal individuals of the same age and gender.

Right anterior cingulate gyrus

Right and total frontal lobe

Right and total superior frontal gyrus

Right and total middle frontal gyrus

Right inferior frontal gyrus

Right and total lateral orbital frontal gyrus

Right medial orbital frontal gyrus

These findings are markedly abnormal corresponds directly to the areas of most pronounced posttraumatic encephalomalacia with permanent liquefied brain tissue and scarring as well as old blood products and hemosiderin related to a direct impaction injury of the right brain/frontal lobe against the skull.

A NeuroQuant triage brain atrophy study was conducted, revealing statistically significant increase in brain volume in the following segments, which fall above the 95th percentile compared to a database of normal individuals of the same age and gender.

Left and total temporal lobe

Left and total entorhinal cortex

Left parahippocampal gyrus

Left and total amygdala

Left and total fusiform gyrus

Left middle temporal gyrus

Left inferior temporal gyrus

Left, right, total temporal pole

Right parietal lobe

Left, right, total superior parietal lobule

Left inferior frontal gyrus

Patient: XXXXXXXX DOB:

MRN#: 209098EVI



Demographics

Patient Name: First: XXXXX Middle: Last: XXXXX XXXXX
Date of Birth: [REDACTED] Gender: M MRN#:209098EVI
Date of Injury: Date of Service: 22-Nov-2024 12:40 PM
Referring Provider / Source: XXXXX, XXXXX

Right lateral orbital frontal gyrus

These findings are abnormal and can be seen in the setting of post traumatic gliosis and scarring or edema suggesting axonal shearing injury as well as a direct impaction injury such as a coup/contrecoup injury (direct brain impact injury).

Previously published studies of patients with mild or moderate TBI often have found atrophy (Hofman, Stapert et al. 2001, MacKenzie, Siddiqi et al. 2002, Ross, Ochs et al. 2012, Toth, Kovacs et al. 2013, Zhou, Kierans et al. 2013, Maller, Thomson et al. 2014, Ross, Ochs et al. 2014, Epstein, Legarreta et al. 2016, Ross, Ochs et al. 2016, Zagorchev, Meyer et al. 2016, Rajesh, Cooke et al. 2017) but occasionally have found abnormal enlargement (Ross, Ochs et al. 2014, Wang, Xie et al. 2015, Govindarajan, Narayana et al. 2016, Ross, Ochs et al. 2016, Ross, Seabaugh et al. 2020, Ross, Seabaugh et al. 2021).

More specifically, outpatients suffering from chronic effects of mild or moderate TBI were found to have some atrophy but more regions of abnormal enlargement (Ross et al., 2014, 2016, 2018b, 2020) (for an example of a patient who had a pattern of cross-sectional brain volumes typical of chronic mild TBI. Multiple brain regions continued to enlarge over time, suggesting that the cross-sectional abnormal enlargement was not due simply to pre-injury enlargement (Ross et al., 2021). Other studies of patients with mild TBI also have found abnormal enlargement (Wang et al., 2015; Govindarajan et al., 2016). These findings were surprising because most studies of brain volume in patients with TBI have found extensive brain atrophy but not enlargement (Bigler, 2005, 2011), but most of those studies were based on patients with severe TBI. Taken together, these studies support the idea that chronic mild TBI has a pathophysiology that is at least somewhat different from that of severe TBI; in other words, it is not simply a milder version of severe TBI.

Several studies of TBI patients found significant correlations between NeuroQuantR or NeuroGageR volume measures and clinical symptoms or outcome. And longitudinal enlargement of the posterior cingulate gyrus was associated with the diagnosis of neuropathic headaches in patients with chronic mild or moderate TBI (Ross et al., 2021); this finding partially replicated an earlier finding by another group (Niu et al., 2020).

The ANDI TBI report uses a normative reference to identify white matter (WM) regions where the subject specific microstructural and macrostructural measures are out of normative range and to create a visual representation of the relation between the observed value and the normative range.

The normative range was calculated based on the distribution of the microstructural and macrostructural measures in the white matter regions of a large sample of healthy-appearing subjects. Datasets constituting the normative reference were chosen to represent the full range of subjects for whom ANDI TBI is applicable. The normative reference is provided as a reference to help clinicians interpret the observed values.

The normative range is based upon 1355 healthy subjects aged between 19 to 83 years old, with 51.3% female / 48.7% male and 77.49% right-handed, 7.75% left-handed and 1.77% ambidextrous and 12.99% unknown handedness. Subjects included in the database are from North America (53.65%), Europe (43.98%), and Worldwide (2.36%). Images were acquired from various MRI

Patient: XXXXXXXX DOB: [REDACTED]

MRN#: 209098EVI

Demographics

Patient Name: First: XXXXX

Middle:

Last: XXXXX XXXXX

Date of Birth: [REDACTED]

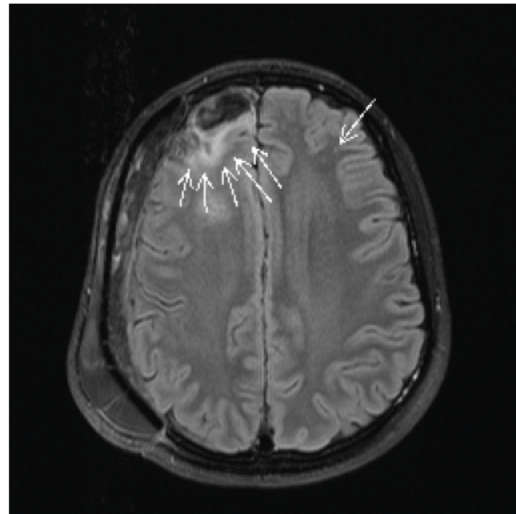
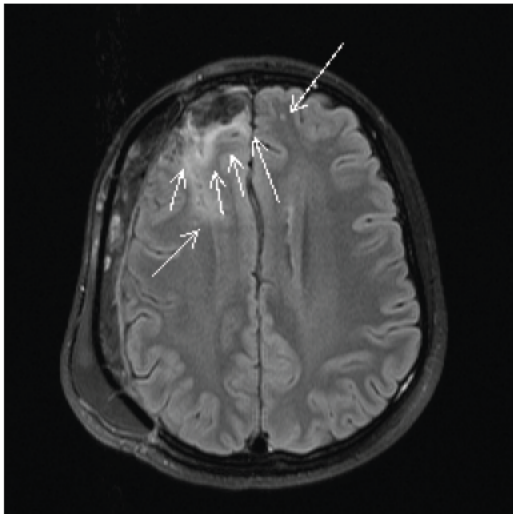
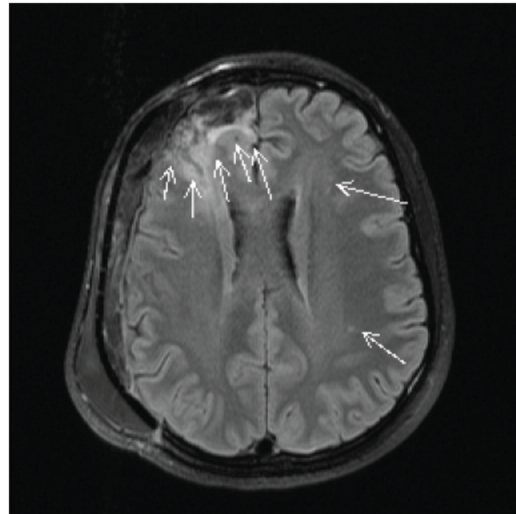
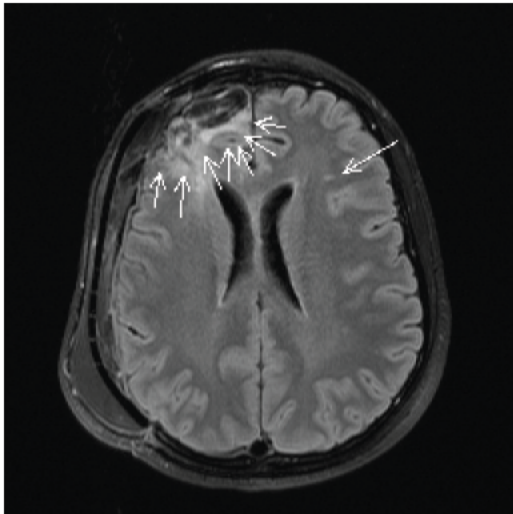
Gender: M

MRN#:209098EVI

Date of Injury:

Date of Service: 22-Nov-2024 12:40 PM

Referring Provider / Source: XXXXX, XXXXX



Patient: XXXXXXXX DOB: [REDACTED]

MRN#: 209098EVI

Demographics

Patient Name: First: XXXXX

Middle:

Last: XXXXX XXXXX

Date of Birth: [REDACTED]

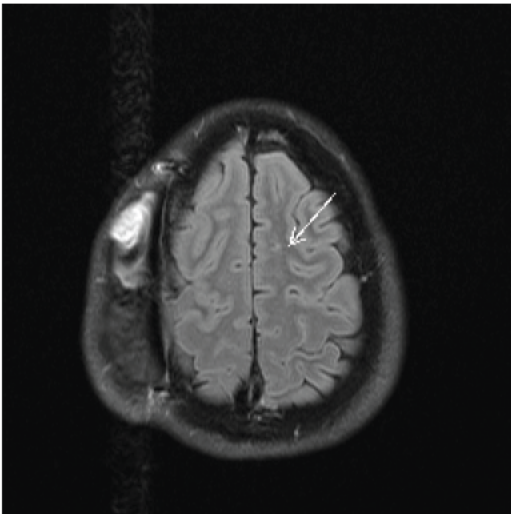
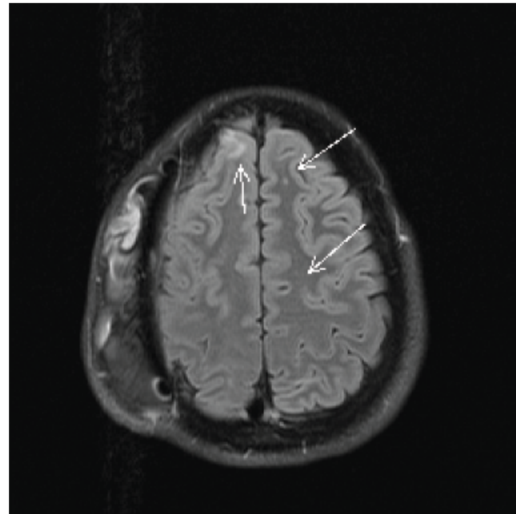
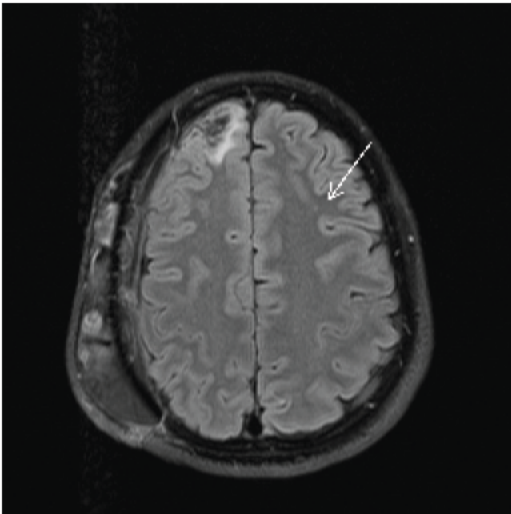
Gender: M

MRN#:209098EVI

Date of Injury:

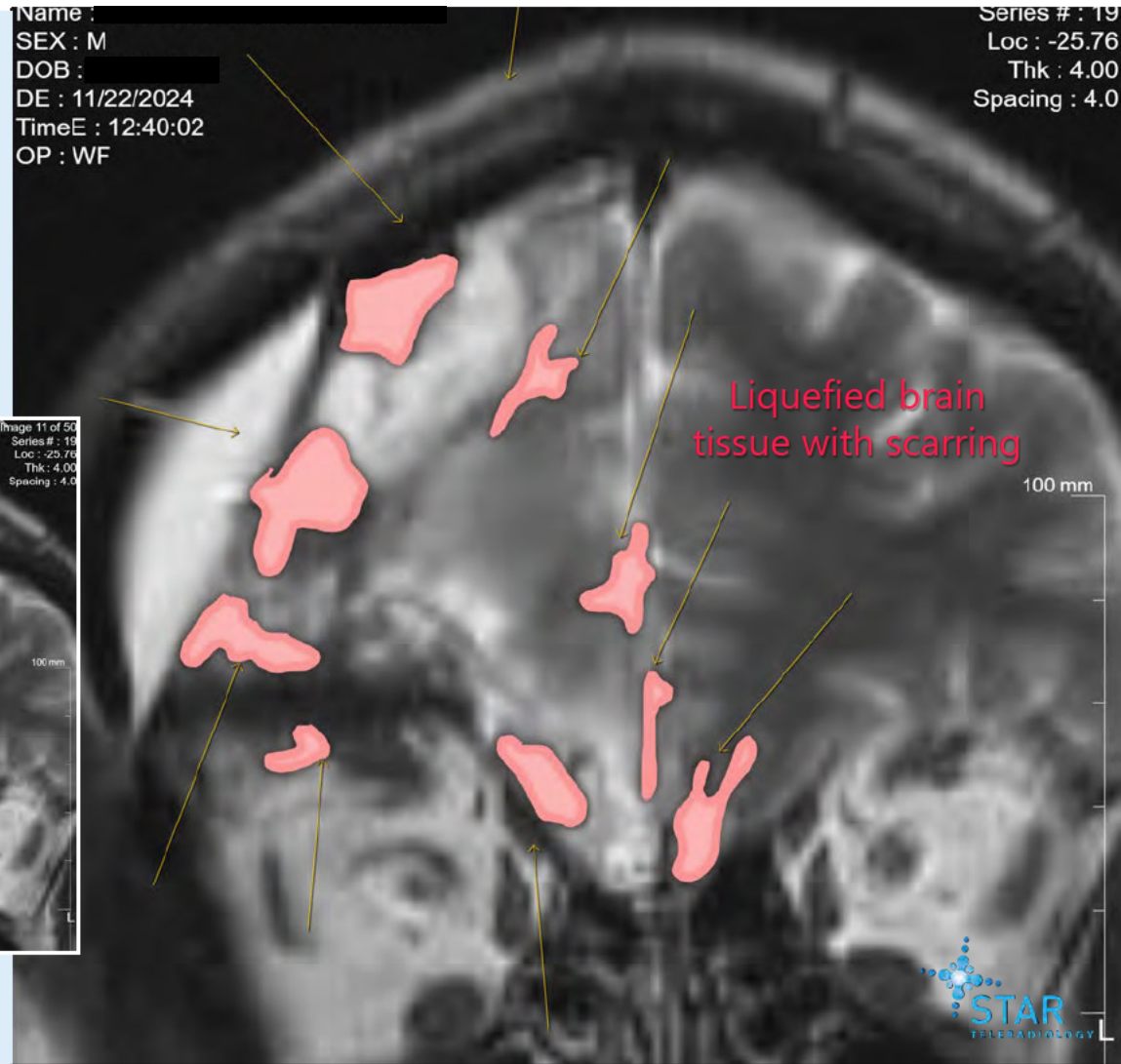
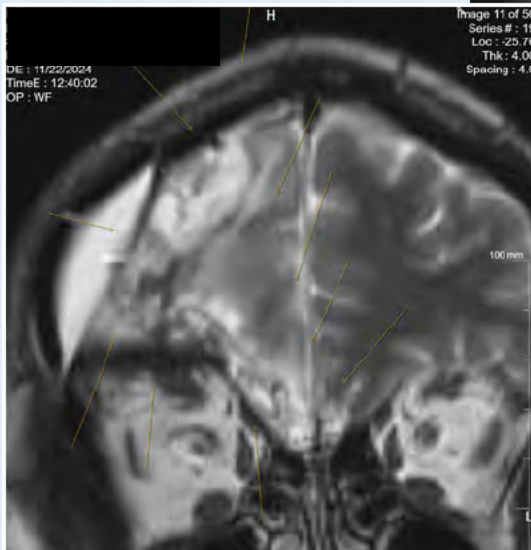
Date of Service: 22-Nov-2024 12:40 PM

Referring Provider / Source: XXXXX, XXXXX



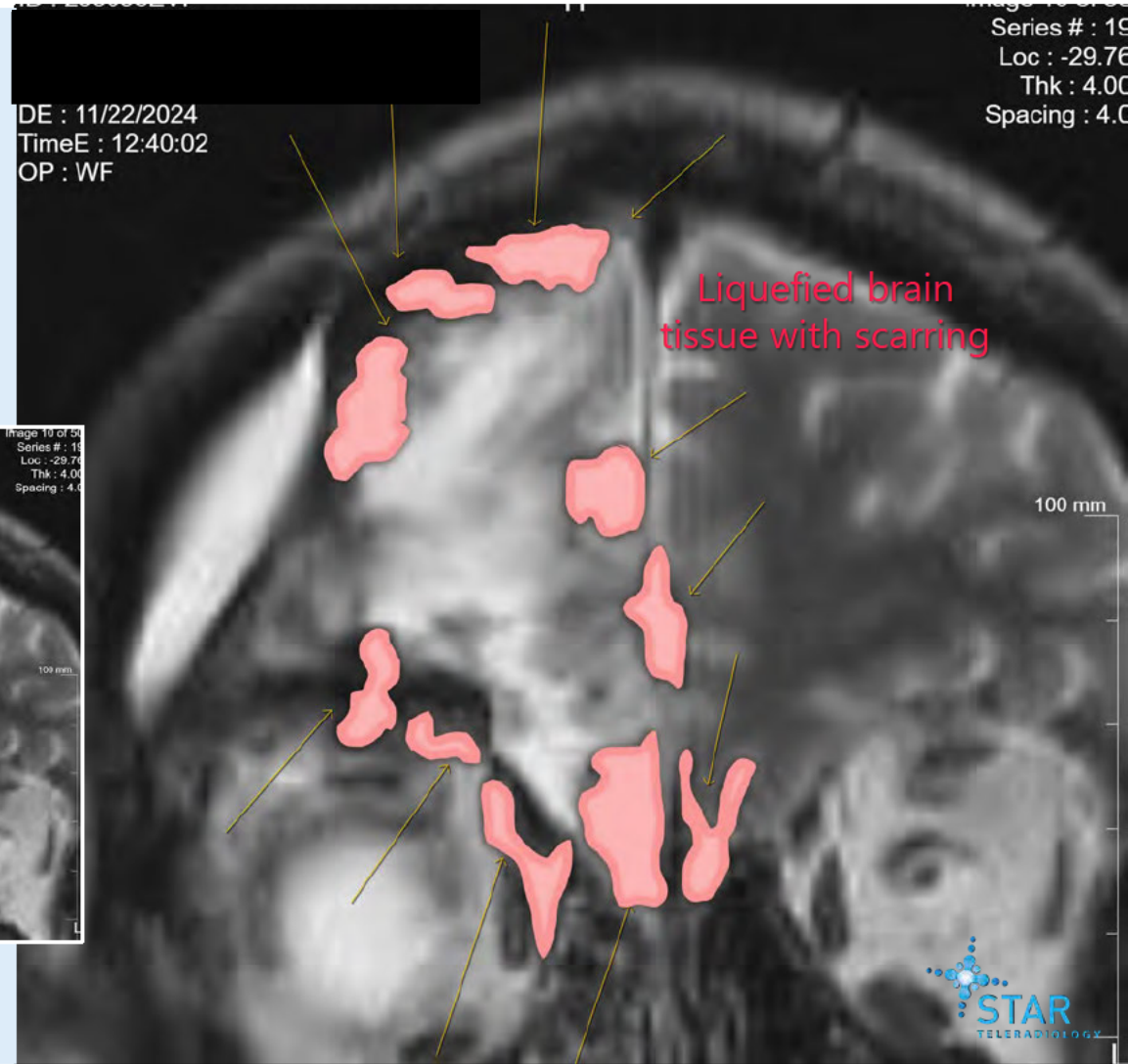
Abnormal Images

Post-traumatic encephalomalacia with permanent liquefied brain tissue.



Abnormal Images

Post-traumatic encephalomalacia with permanent liquefied brain tissue.

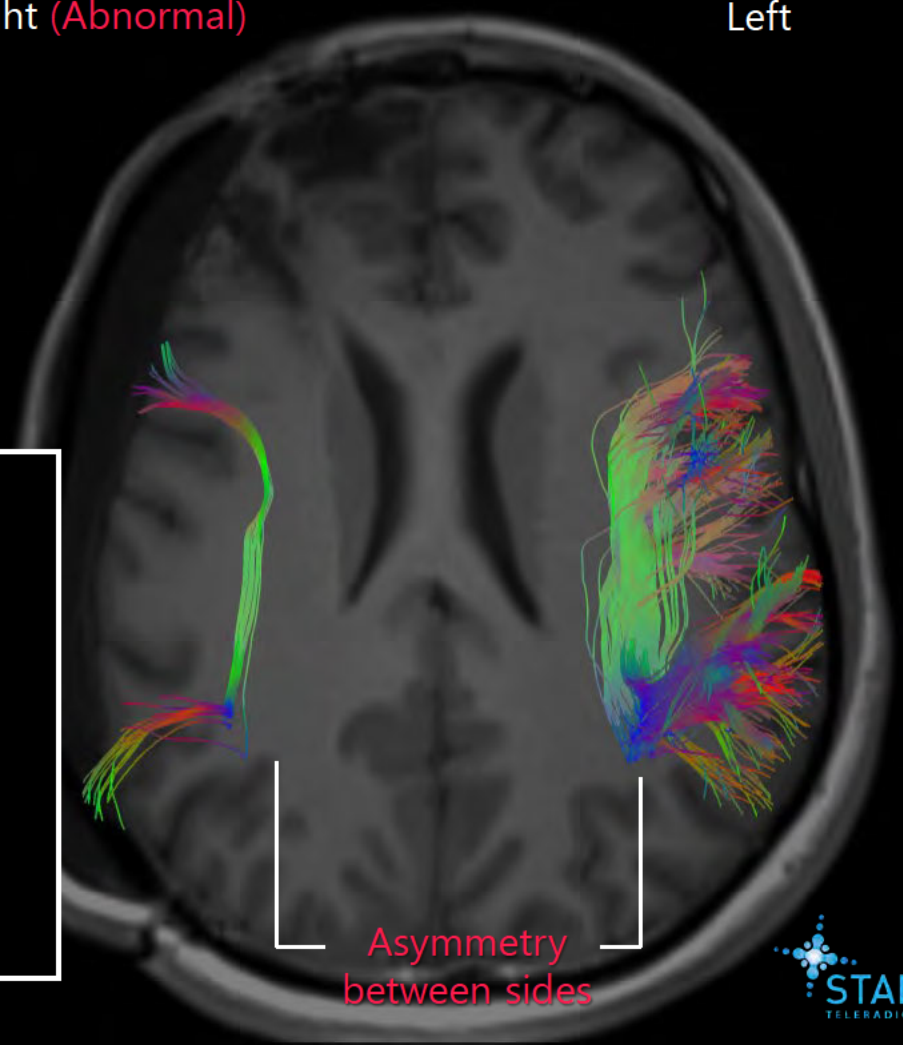
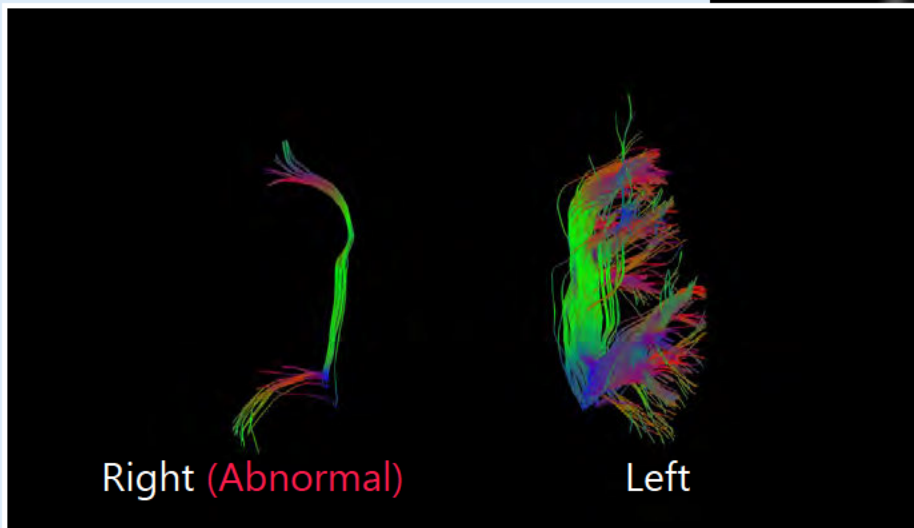


Arcuate Fasciculus (R)

Asymmetric reduced fiber density and disrupted fiber tracts, corresponding to areas with abnormal axonal microstructural properties of the brain consistent with axonal dysfunction most indicative of **traumatic axonal injury.**

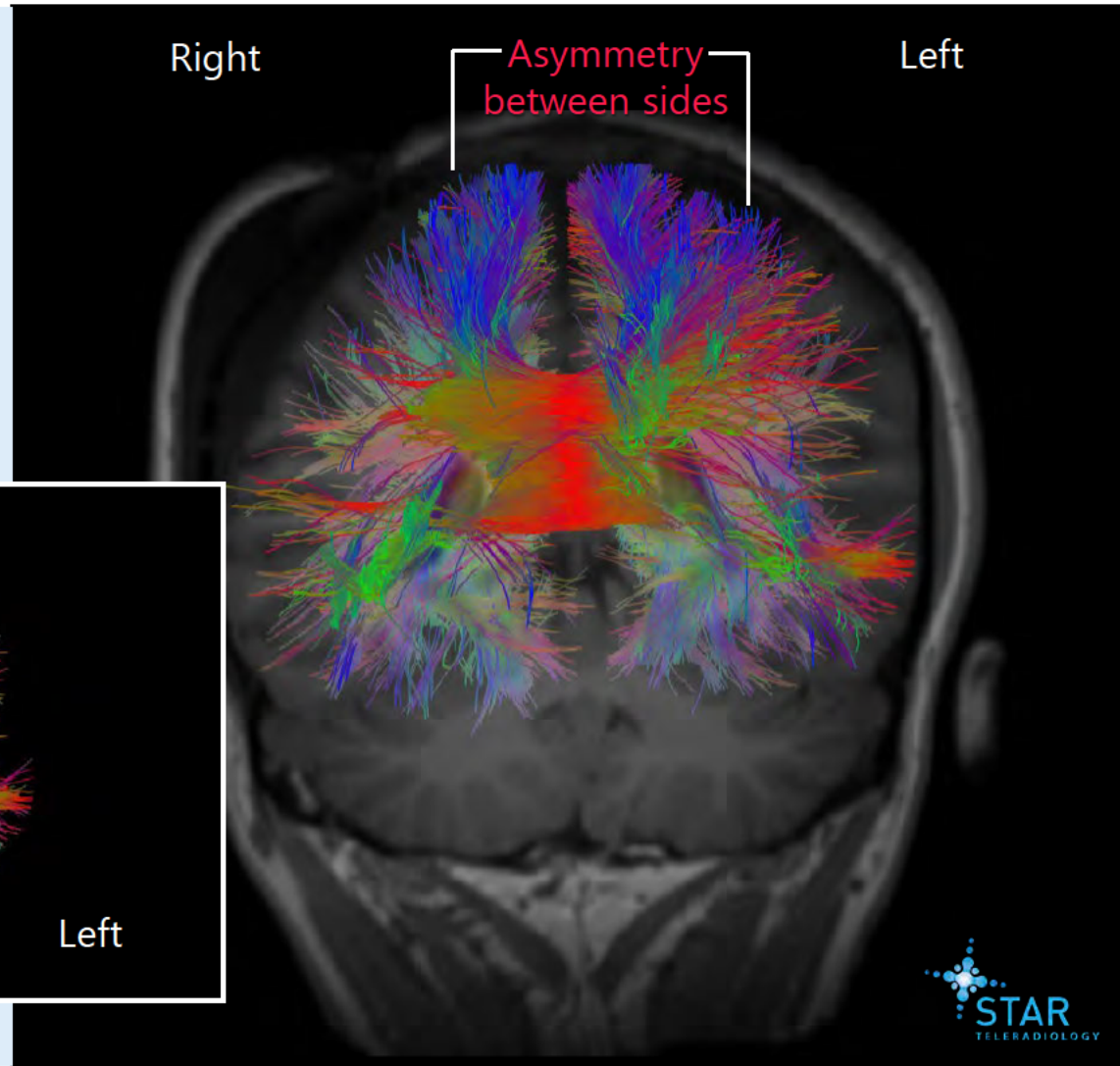
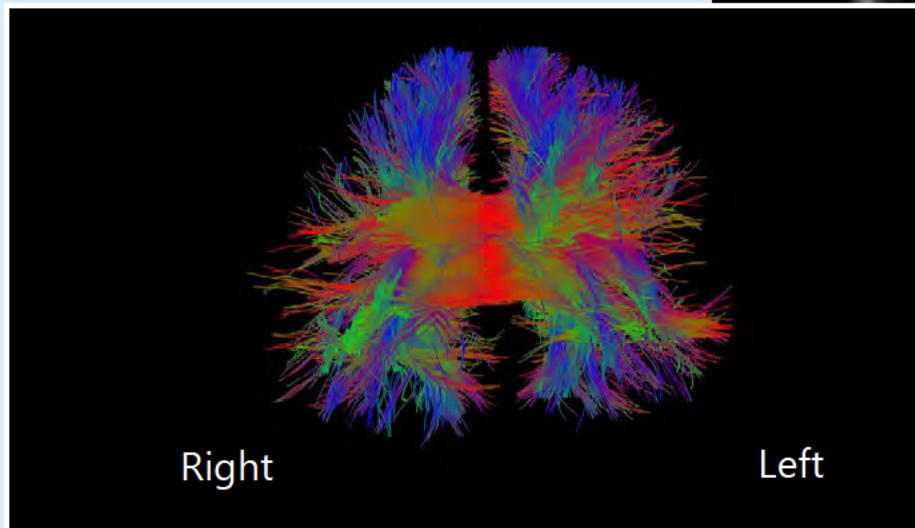
Right (Abnormal)

Left



Corpus Callosum

Irregularities, including **reduced fiber density and disrupted fiber tracts**, corresponding to areas with abnormal **axonal microstructural properties** of the brain consistent with axonal dysfunction commonly seen in traumatic axonal injury.



Star Teleradiology

Patient Name: [REDACTED]
 Study Date: 11/22/2024 12:40 PM
 Study Description: MRI 3D RENDER W/INTRP POSTPRO - DTI VIDEO

Patient Sex: M

Patient DOB: [REDACTED]

NeuroQuant® TBA

Triage Brain Atrophy Report: Single Timepoint

Patient Information

Patient: [REDACTED]
 Referring Physician: [REDACTED]
 Age: 32 Sex: M Patient ID: 209098EVI

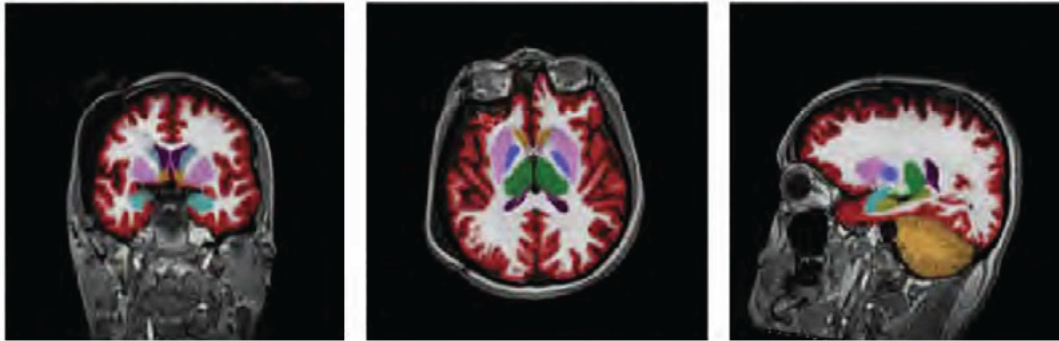
Report Information

Scan Date: 2024-11-22

Site Information

Star Teleradiology
 B13 609 2579

Brain Structure Visualization



Brain Structure Volumes

Brain Volumes	Volume (cm³)	Normative Percentile
Whole Brain	1298	44
Cortical Gray Matter	540	43
Cerebral White Matter	513	37
Cerebral WM Hypointensities*	0.19	-

Regional Brain Structures	Normative Percentiles		
	Left	Right	Total
Ventricles	23	40	31
Cerebellum	61	84	74
Brainstem	-	-	79
Deep Gray Nuclei			
- Putamen	87	34	63
- Thalamus	94	48	74
- Caudate	80	11	41
Cingulate	74	6	26
- Anterior Cingulate Gyrus	87	1	16
- Posterior Cingulate Gyrus	12	38	19

*White matter hypointensities are abnormally low signal intensity regions within the white matter as observed on a T1-weighted MRI scan.

Color Code Key:

- A structure is below the 5th percentile OR a ventricle is above the 95th percentile.
- A structure is above the 95th percentile OR a ventricle is below the 5th percentile.

Regional Lobe Analysis	Normative Percentiles		
	Left	Right	Total
Temporal Lobe	99	89	99
- Hippocampus	84	75	80
- Entorhinal Cortex	99	95	99
- Parahippocampal Gyrus	99	58	91
- Amygdala	99	99	99
- Fusiform Gyrus	99	20	96
- Superior Temporal Gyrus	99	42	63
- Middle Temporal Gyrus	99	53	86
- Inferior Temporal Gyrus	97	95	98
- Temporal Pole	99	99	99
Parietal Lobe	70	96	89
- Primary Sensory Cortex	61	0	30
- Superior Parietal Lobule	97	99	99
- Supramarginal Gyrus	10	16	9
Frontal Lobe	34	1	1
- Primary Motor Cortex	62	77	43
- Superior Frontal Gyrus	6	2	2
- Middle Frontal Gyrus	17	1	1
- Inferior Frontal Gyrus	96	1	9
- Lateral Orbitofrontal Gyrus	34	1	1
- Medial Orbitofrontal Gyrus	82	1	15
Occipital Lobe	49	74	78
- Medial Occipital	38	64	50
- Lateral Occipital	61	95	92

Star Teleradiology

Patient Name: [REDACTED]
Study Date: 11/22/2024 12:40 PM
Study Description: MRI 3D RENDER W/INTRP POSTPRO - DTI VIDEO

Patient Sex: M

Patient DOB: [REDACTED]

NeuroQuant[®] Morphometry

General Morphometry Report: Single Timepoint

Patient Information

Patient: [REDACTED]
Referring Physician: [REDACTED]
Age: 32 Sex: M Patient ID: 209098LVI

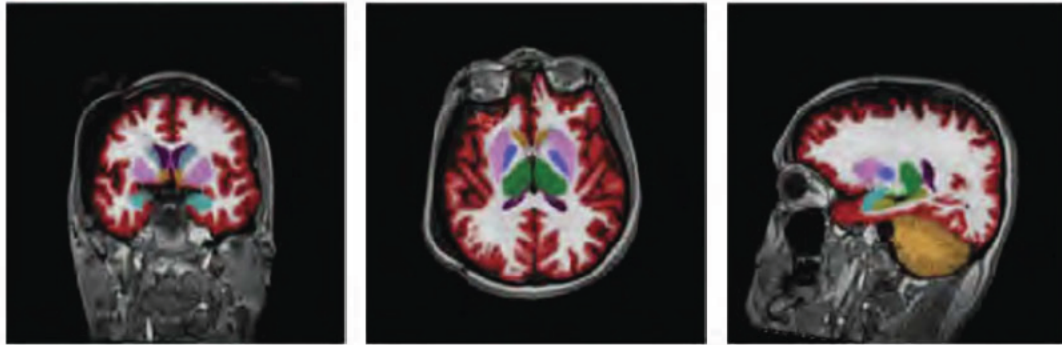
Report Information

Scan Date: 2024-11-22

Site Information

Star Teleradiology
813 609 2579

Brain Structure Visualization



Brain Structure Volumes

Intracranial Volume (ICV) (cm³) 1716

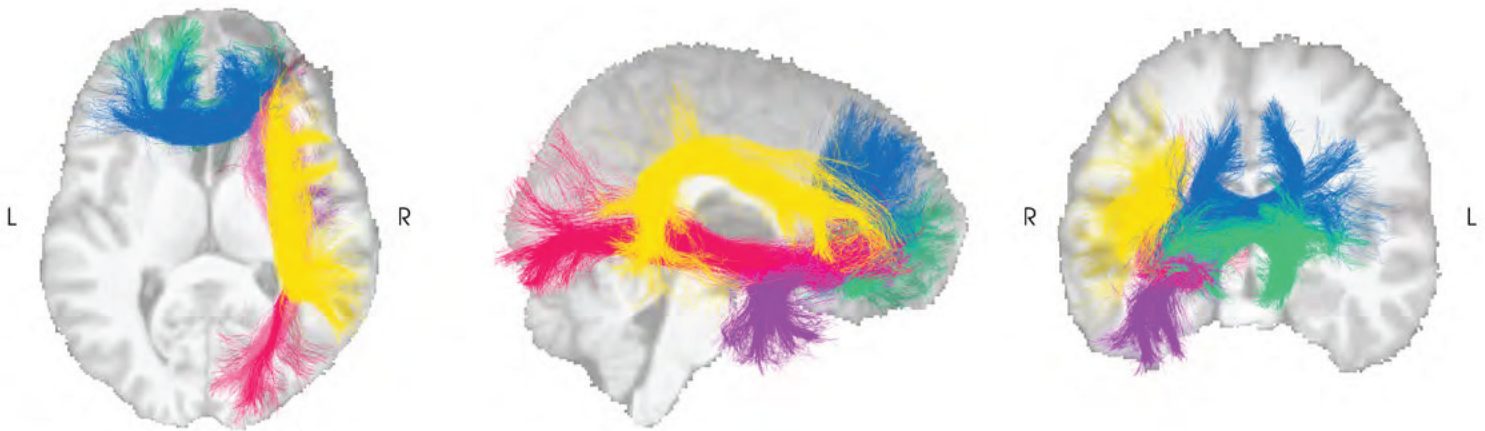
Brain Structure	LH Volume (cm ³)	LH Volume (% of ICV)	RH Volume (cm ³)	RH Volume (% of ICV)	Asymmetry Index (%) [*]
Forebrain Parenchyma	586	34.2	531	31	0.79
Cortical Gray Matter	283	16.5	257	15	9.5
Superior Lateral Ventricles	7.53	0.44	8.14	0.47	-7.9
Inferior Lateral Ventricles	0.39	0.02	1.05	0.06	-91.1
Hippocampi	4.18	0.24	4.2	0.24	-0.43
Amygdalae	3.04	0.18	2.80	0.17	5.54
Caudates	3.48	0.2	2.86	0.17	19.5
Putamina	7.13	0.42	5.94	0.35	18.2
Pallidums	1.37	0.06	1.09	0.06	22.6
Thalami	9.48	0.55	8.63	0.5	9.41
Cerebellum	76.1	4.43	79.1	4.61	-3.86

^{*}The Asymmetry Index is defined as the percentage difference between left and right volumes divided by their mean.

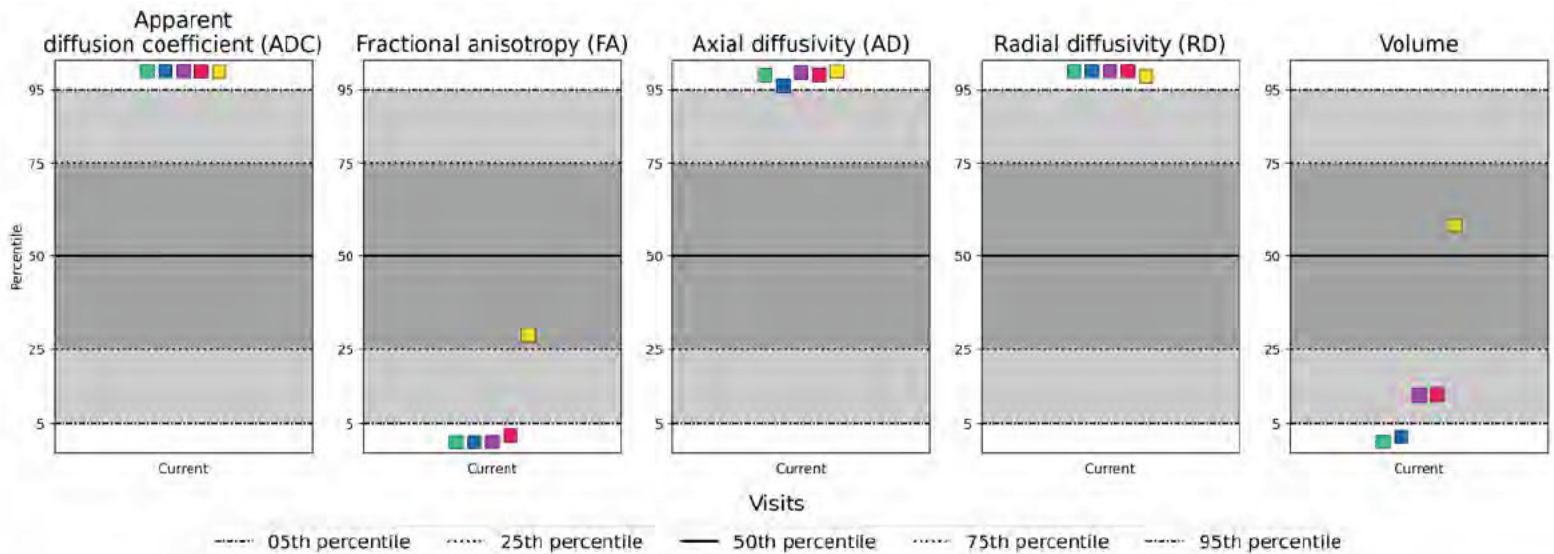
Created
11/22/2024 12:40 PM



Top 5 out of normative range bundles

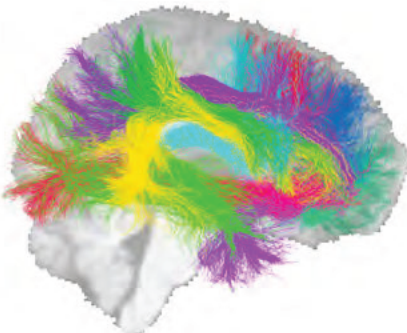


As displayed in the image above, the top 5 out of normative range bundles in terms of microstructural measures are the **Anterior genu**, **Middle genu**, **Uncinate fasciculus right**, **Inferior fronto-occipital fasciculus right**, **Arcuate fasciculus right**. They are mainly situated in the right hemisphere.



Analysis overview

As displayed in the left image, there are 33.3 % (11/33) bundles out of the normative range in terms of microstructural measures. The majority of the bundles out of the normative range are in the right hemisphere. There are 4 bundles out of the normative range in terms of volume. The complete list of bundles out of the normative is presented on the next pages.



Regions < 5th or > 95th percentile for microstructural measures

Brain structure	Apparent diffusion coefficient (ADC) (percentile)	Fractional anisotropy (FA) (percentile)	Axial diffusivity (AD) (percentile)	Radial diffusivity (RD) (percentile)	Volume (percentile)
Anterior genu	100.000	0.000	98.770	100.000	0.041
Middle genu	100.000	0.002	95.975	100.000	1.328
Uncinate fasciculus right	100.000	0.009	99.437	100.000	12.610
Inferior fronto-occipital fasciculus right	99.919	1.789	98.856	99.949	12.765
Arcuate fasciculus right	99.695	28.876	99.871	98.542	58.348
Superior longitudinal fasciculus 3 right	99.487	15.342	99.700	98.683	37.408
Fornix right	99.556	7.496	99.467	99.547	9.372
Frontal aslant tract right	99.005	24.293	99.128	97.624	0.027
Superior longitudinal fasciculus 2 right	96.649	43.360	98.005	93.366	5.869
Inferior longitudinal fasciculus right	96.789	19.461	95.992	95.437	69.049
Posterior genu	95.743	30.120	93.826	94.149	0.170

Regions < 5th or > 95th percentile for volume only

Brain structure	Apparent diffusion coefficient (ADC) (percentile)	Fractional anisotropy (FA) (percentile)	Axial diffusivity (AD) (percentile)	Radial diffusivity (RD) (percentile)	Volume (percentile)
Anterior body	90.701	67.553	94.348	80.707	1.862
Frontal aslant tract left	70.164	56.607	72.354	65.004	2.498
Arcuate fasciculus left	76.371	63.541	85.666	61.361	96.459
Optic radiation right	88.961	22.442	88.703	86.744	99.643

Asymmetry ratio

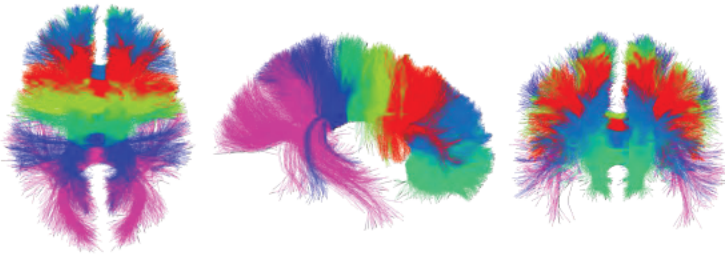
The asymmetry ratio compares the right side to the left side.

Brain structure	Apparent diffusion coefficient (ADC)	Fractional anisotropy (FA)	Axial diffusivity (AD)	Radial diffusivity (RD)
Arcuate fasciculus	10.6% (99.1 perc)	-8.9% (7.8 perc)	8.0% (99.5 perc)	13.0% (97.9 perc)
Cingulum	3.8% (97.8 perc)	-14.6% (0.1 perc)	-2.1% (46.8 perc)	9.1% (99.8 perc)
Corona radiata	2.4% (56.7 perc)	-1.1% (44.0 perc)	1.8% (50.2 perc)	3.1% (59.9 perc)
Frontal aslant tract	7.7% (99.3 perc)	-7.5% (4.6 perc)	6.3% (99.6 perc)	8.9% (98.2 perc)
Fornix	20.1% (99.4 perc)	-17.8% (0.9 perc)	17.3% (99.3 perc)	22.2% (99.4 perc)
Inferior fronto-occipital fasciculus	8.9% (100.0 perc)	-9.2% (2.2 perc)	5.3% (99.6 perc)	12.2% (99.9 perc)
Inferior longitudinal fasciculus	5.0% (93.1 perc)	-6.0% (6.3 perc)	2.8% (87.0 perc)	7.1% (93.9 perc)
Optic radiation	2.6% (88.0 perc)	-0.1% (43.8 perc)	2.8% (92.4 perc)	2.3% (81.2 perc)
Pyramidal tract	2.1% (59.0 perc)	-2.5% (34.6 perc)	0.8% (44.8 perc)	3.7% (65.9 perc)
Superior longitudinal fasciculus 1	4.7% (99.5 perc)	-4.9% (24.5 perc)	2.8% (91.6 perc)	6.4% (98.2 perc)
Superior longitudinal fasciculus 2	9.5% (99.8 perc)	-6.8% (2.1 perc)	7.1% (99.0 perc)	11.8% (99.8 perc)
Superior longitudinal fasciculus 3	12.4% (99.5 perc)	-14.9% (0.3 perc)	8.6% (99.6 perc)	15.9% (99.1 perc)
Uncinate fasciculus	13.8% (100.0 perc)	-34.9% (0.0 perc)	4.3% (96.8 perc)	21.0% (100.0 perc)

UDI: (01)00754016387111(10)ANDiv1.4.0
 ANDI is a regulated medical device in the USA.
 Click [here](#) to learn more.

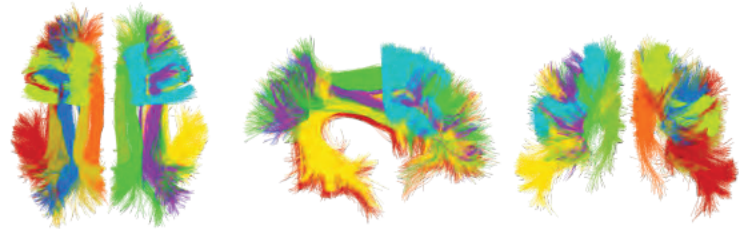
Bundles index

Corpus callosum



- [Anterior genu](#)
- [Middle genu](#)
- [Posterior genu](#)
- [Anterior body](#)
- [Posterior body](#)
- [Isthmus](#)
- [Splenium](#)

Association dorsal bundles



Arcuate fasciculus

- [Left](#) ■ [Right](#)

Cingulum

- [Left](#) ■ [Right](#)

Frontal aslant tract

- [Left](#) ■ [Right](#)

Superior longitudinal fasciculus (SLF)

- SLF 1 ■ [Left](#) ■ [Right](#)

- SLF 2 ■ [Left](#) ■ [Right](#)

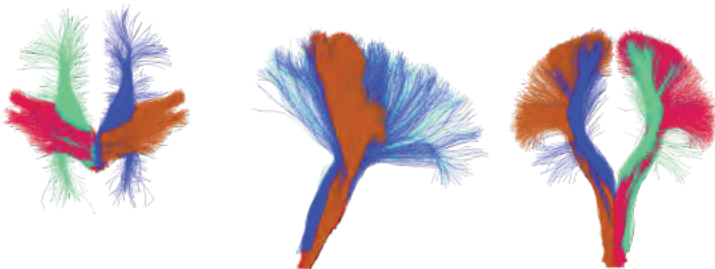
- SLF 3 ■ [Left](#) ■ [Right](#)

Fornix



- [Left](#) ■ [Right](#)

Projection bundles



Corona radiata

- [Left](#) ■ [Right](#)

Pyramidal tract

- [Left](#) ■ [Right](#)

Association ventral bundles



Inferior fronto-occipital fasciculus

- [Left](#) ■ [Right](#)

Inferior longitudinal fasciculus

- [Left](#) ■ [Right](#)

Optic radiation

- [Left](#) ■ [Right](#)

Uncinate fasciculus

- [Left](#) ■ [Right](#)

This glossary lists a brief description of each measure and bundle. For more information on measures and bundles, please see the user manual.

Measures

Apparent diffusion coefficient (ADC): The ADC is derived from the Diffusion Tensor model (DT). ADC is equivalent to the Mean Diffusivity (MD). Represents the mean diffusion phenomenon along all acquired directions. ADC is high in Cerebrospinal Fluid and generally lower in structured tissue.

Fractional anisotropy: The Fractional Anisotropy (FA) is derived from the Diffusion Tensor model (DT). Measures the anisotropy of diffusion from 0 to 1. Zero (0) represents completely isotropic diffusion (eg: in CSF) and one (1) means completely anisotropic diffusion along a specific direction.

Axial diffusivity: The Axial Diffusivity (AD) is derived from the Diffusion Tensor model (DT). Represents the amplitude of the main orientation of the tensor. A larger value indicates that the diffusion process was strongly aligned with this main direction.

Radial diffusivity: The Radial Diffusivity (RD) is derived from the Diffusion Tensor model (DT). Represents the average amplitude of the second and third direction of the tensor. The greater the value, the more diffusion was perpendicular to the main diffusion direction.

Volume: The volume of the bundle or white matter, in cubic centimeters, as measured in MNI space. This is a macrostructural measure.

Bundles

Whole white matter: This is not a specific bundle. It represents a safe mask of the white matter, as a global region of analysis. Only voxels with high confidence of being white matter are included in this mask.

Corpus callosum genu: The corpus callosum is a set of commissural fibers connecting both hemispheres. ANDI subdivides the corpus callosum in 7 anatomically distinct bundles, based on the work of Keshavan et al, 2002. The bundles are, in order from the most anterior to most posterior localization:

- The Anterior Genu
- The Middle Genu
- The Posterior Genu
- The Anterior Body
- The Posterior Body
- The Isthmus
- The Splenium

Fornix: The fornix is a branching bundle which is considered to be the major output tract from the hippocampus. The fornix is subdivided into its left and right sections.

Projection bundles: Projection bundles consist of white matter bundles that connect the cortex to the lower part of the brain and / or the spinal cord. ANDI reconstructs the following projection bundles:

- *Corona Radiata:* Consist of axons connecting the cortex to the brain stem. ANDI extracts the left and right sections of the Corona Radiata.
- *Pyramidal Tract:* Includes the corticobulbar tract and the corticospinal tract, connecting the cortex to either the brain stem or the spinal cord. ANDI extracts the left and right Pyramidal Tract.

Association dorsal bundles: Association dorsal bundles include the Arcuate Fasciculus, the Cingulum and the Frontal Aslant Tract, each subdivided into its left and right components. They also include the Superior Longitudinal Fasciculus, which is subdivided into 3 distinct parts, each lateralized.

- *Arcuate Fasciculus (AF):* The AF connects the caudal temporal cortex and inferior frontal lobe, with connections to Broca's area (BA 44). ANDI extracts both the left and right AF.
- *Cingulum (Cg):* Part of the limbic system, it connects the cingulate gyrus to the entorhinal cortex. ANDI extracts both the left and right Cg.
- *Frontal Aslant Tract (FAT):* Bundle that connects the inferior frontal gyrus to the supplementary motor cortex and the lateral superior frontal gyrus. ANDI extracts both the left and right FAT.
- *Superior Longitudinal Fasciculus (SLF):* The SLF is a large fiber bundle that connects the frontal, parietal, temporal and occipital lobes. ANDI subdivides it in 3 distinct bundles, based on their spatial localization and connection patterns.
 - *SLF 1:* Connects the superior and medial parietal cortex to the dorsal and medial cortex of the frontal lobe. Left and right SLF 1 are extracted.
 - *SLF 2:* Links the caudal-inferior parietal cortex to the dorsolateral region of the prefrontal cortex. Left and right SLF 2 are extracted.
 - *SLF 3:* Connects the prefrontal cortex to the supramarginal gyrus. Left and right SLF 3 are extracted.

Association ventral bundles: Association ventral bundles include Inferior Fronto-Occipital fasciculus, the Inferior Longitudinal Fasciculus, the Optic Radiations and the Uncinate Fasciculus. Each of these bundles are separated in their left and right components.

- *Inferior Fronto-Occipital Fasciculus (IFOF):* The IFOF connects the parietal and occipital lobes to the frontal lobe. ANDI extracts both the left and right IFOF.
- *Inferior Longitudinal Fasciculus (ILF):* The ILF links the extrastriate cortex of the occipital lobe to the anterior temporal lobe (temporal surface). ANDI extracts both the left and right ILF.
- *Optic Radiations (OR):* The OR is a fiber bundle connecting the primary visual cortex to the lateral geniculate nucleus.
NOTE: ANDI's reconstruction of the optic radiation does not reach the optic chiasma nor the eyes region. ANDI extracts both the left and right OR.
- *Uncinate fasciculus (UF):* The UF is part of the limbic system and links parts of the anterior temporal lobe with the inferior frontal gyrus, as well as with lower parts of the frontal lobe. ANDI extracts both the left and right UF.

UDI: (01)00754016387111(10)ANDIv1.4.0
ANDI is a regulated medical device in the USA.
Click [here](#) to learn more.